Journal of Materials Chemistry A

Accepted Manuscript

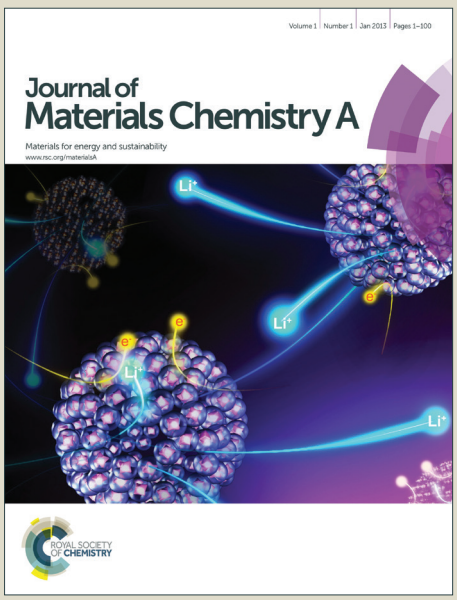

This is an *Accepted Manuscript*, which has been through the Royal Society of Chemistry peer review process and has been accepted for publication.

Accepted Manuscripts are published online shortly after acceptance, before technical editing, formatting and proof reading. Using this free service, authors can make their results available to the community, in citable form, before we publish the edited article. We will replace this *Accepted Manuscript* with the edited and formatted *Advance Article* as soon as it is available.

You can find more information about *Accepted Manuscripts* in the Information for Authors.

Please note that technical editing may introduce minor changes to the text and/or graphics, which may alter content. The journal's standard Terms & Conditions and the Ethical guidelines still apply. In no event shall the Royal Society of Chemistry be held responsible for any errors or omissions in this *Accepted Manuscript* or any consequences arising from the use of any information it contains.

ROYAL SOCIETY OF CHEMISTRY

www.rsc.org/materialsA

Journal Name

ARTICLE

Porous nitrogen-doped carbon-immobilized bimetallic nanoparticles as highly efficient catalysts for hydrogen generation from hydrolysis of ammonia borane

Received 00th January 20xx,
Accepted 00th January 20xx

DOI: 10.1039/x0xx00000x

www.rsc.org/

Lingling Guo, Xiaojun Gu,* Kai Kang, Yanyan Wu, Jia Cheng, Penglong Liu, Tianshu Wang and Haiquan Su*

Two N-doped carbon materials, N-doped Vulcan XC-72 carbon labelled as NXC and graphite carbon nitride labelled as C_3N_4, were selected as supports to prepare a series of bimetallic AuM (M = Co, Ni) nanoparticles (NPs) using three different reduction ways towards mixed metal ions $AuCl_4^-$ and M^{2+}, and then the as-synthesized supported bimetallic AuM NPs were used as catalysts for hydrolytic dehydrogenation of ammonia borane (NH_3BH_3). All the catalysts exhibited high dispersion and small size of bimetallic NPs; however, they exhibited remarkably different catalytic activities featuring total turnover frequency (TOF) values from 6.4 to 42.1 $mol_{H2}{\cdot}mol_{cat}^{-1}{\cdot}min^{-1}$. Among all the catalysts, the NXC-immobilized AuCo NPs through in situ synthesis using $NaBH_4$ and NH_3BH_3 as reductants exhibited the highest activity with a total TOF value of 42.1 $mol_{H2}{\cdot}mol_{cat}^{-1}{\cdot}min^{-1}$, which was among the highest values for Co-based catalysts ever reported for hydrolytic dehydrogenation of NH_3BH_3. This remarkably enhanced activity may be attributed to the synergistic effect of N-doped NXC support and AuCo NPs and the resulting highly efficient activation of N-B bond in NH_3BH_3. In addition, the AuCo catalysts showed good recyclability, demonstrating that they had high stability/durability.

1. Introduction

Hydrogen has been considered as a globally accepted energy carrier to satisfy the increasing demand for sustainable and clean energy supply.[1] The safe and efficient storage and production of hydrogen are still the challenging technologies on the way towards a fuel-cell-based hydrogen economy.[2] Currently, chemical hydrides have attracted much attention owing to their high gravimetric and volumetric storage capacity.[3] Among them, despite the relatively high cost, ammonia borane (NH_3BH_3) is still regarded as one of the most promising candidates for the storage of hydrogen since it is stable and non-toxic at ambient temperature and has a high hydrogen content of 19.6 wt%, outstripping that of gasoline.[4] In comparison with the pyrolysis of NH_3BH_3 to generate H_2, where the high temperature is required, H_2 is not fully released and the rate of hydrogen generation is low, the hydrolysis of NH_3BH_3 ($NH_3BH_3 + 2H_2O \rightarrow NH_4BO_2 + 3H_2$) can proceed rapidly with 100 % of H_2 selectivity at room temperature in the presence of a suitable heterogeneous catalyst.[5]

To date, three types of active metals, noble metals such as Pt, Ru and Pd, inexpensive first-row transition metals such as Fe, Co and Ni and their bimetallic composites, have been developed for hydrogen generation from hydrolysis of NH_3BH_3.[6] Recently, the microstructures of the bimetallic nanoparticles (NPs) such as alloy and core-shell morphologies have been reported to influence the performance of catalysts in various fields including the hydrolysis of NH_3BH_3.[7] In addition, many investigations on hydrolysis of NH_3BH_3 have revealed that the catalytic performance, especially the activity, is highly related with the dispersity and size of active metal nanoparticles (NPs).[8] So in order to acquire the high activity in hydrolytic dehydrogenation of NH_3BH_3, the catalysis system involving supported metal catalysts has been explored in recent years.[9] More recently, the route regarding photocatalysis has been introduced to the hydrolysis of NH_3BH_3 using porous semiconductor-supported Au-Co nanoparticles, which display exceedingly high activity.[10] However, how to remarkably enhance the activity of supported catalysts in hydrolysis of NH_3BH_3 without light still remains a challenge due to the difficulty in rationally synthesizing highly dispersed metal NPs with different microstructures and tuning the interactions between supports and active metal NPs.[11] To this end, the selection of supports is the key issue.

Herein, we reported a series of porous functionalized carbon-immobilized AuM (M = Co, Ni) NPs using three different reduction ways towards mixed metal ions $AuCl_4^-$ and M^{2+}, which exhibited remarkably different catalytic activity for

Inner Mongolia Key Laboratory of Coal Chemistry, School of Chemistry and Chemical Engineering, Inner Mongolia University, Hohhot 010021, China. E-mail: xiaojun.gu@yahoo.com, haiquansu@yahoo.com; Fax: +86-471-499-2981; Tel: +86-471-499-2981

† Electronic Supplementary Information (ESI) available: TEM, EDS, XRD, IR, BET, XPS, and TOF data; the experimental results for H_2 generation from NH_3BH_3. See DOI: 10.1039/x0xx00000x

Journal of Materials Chemistry A Accepted Manuscript

hydrolysis of NH_3BH_3. For convenience, Vulcan XC-72 carbon was labelled as XC. N-doped Vulcan XC-72 carbon labelled as NXC and graphite carbon nitride labelled as C_3N_4 were selected as supports on the basis of the four considerations. Firstly, carbon materials are cheap in the resource and have various functional applications.[12] Secondly, metal NPs deposited on bare carbon materials easily leach during catalytic processes owing to the weak interaction between the metal NPs and the carbon surface.[13] Thirdly, the N-doping in carbon could not only change the physicochemical and electronic properties of carbon, but also serve as basic or coordination sites to stabilize the small metal NPs or activate catalytic substrates.[14] Fourth, bare carbon and two different N-doped carbon materials provided us a chance to explore the effect of supports with different structures on catalytic activities. It was interesting that through tuning the structures of N-doped carbon supports and the reduction ways towards mixed metal ions in the synthesis of catalysts, the activity for hydrogen generation from hydrolysis of NH_3BH_3 was remarkably enhanced, featuring the total turnover frequency (TOF) values from 6.4 to 42.1 $mol_{H2}{\cdot}mol_{cat}^{-1}{\cdot}min^{-1}$.

2. Experimental section

2.1 Chemicals

All chemicals were commercial and were employed with no further purification. Cobalt (II) chloride hexahydrate ($CoCl_2{\cdot}6H_2O$, Sinopharm Chemical Reagent Co. Ltd, >99%), nickel (II) chloride hexahydrate ($NiCl_2{\cdot}6H_2O$, Tianjin Fengchuan Chemical Reagent Technologies Co. Ltd, >99%), tetrachloroauric (III) acid ($HAuCl_4{\cdot}4H_2O$, Tianjin Fengchuan Chemical Reagent Technologies Co. Ltd, >99%), sodium borohydride ($NaBH_4$, J&K Chemical, 98%), NH_3BH_3 (Aldrich, 97%), XC (Cabot Chemical Co. Ltd), glacial acetic acid (CH_3COOH, Tianjin Fengchuan Chemical Reagent Technologies Co. Ltd, $\geqslant$ 99.5%), pyrrole (C_4H_5N, Sigma-Aldrich, 98%), hydrogen peroxide (H_2O_2, Tianjin Fengchuan Chemical Reagent Technologies Co. Ltd, $\geqslant$ 30.0%), L-lysine ($C_6H_{14}N_2O_2$, J&K Chemical, 98%), n-octane ($CH_3(CH_2)_6CH_3$, Alfa Aesar Chemical Co. Ltd, $\geqslant$98%), Tetraethyl orthosilicate ($C_8H_{20}O_4Si$, Sinopharm Chemical Reagent Co. Ltd, $\geqslant$99%), ammonium hydrogen difluoride (NH_4HF_2, J&K Chemical, 98%) and cyanamide (CN_2H_2, Alfa Aesar Chemical Co. Ltd, $\geqslant$98%) were obtained. Deionized water was used in all experiments.

2.2 Synthesis and catalytic study

For the synthesis of NXC, 5 mL of glacial acetic acid was added to 45 mL of deionized water containing XC (0.500 g) under vigorously stirring. After 4 hours, pyrrole (0.334 g) was introduced into the suspension with sonication for 20 min and stirred for 2 hours. Then 5 mL of hydrogen peroxide was added into the mixture. After stirring for 12 hours, the solid was filtered from the solution, washed with deionized H_2O for several times, and then dried in vacuum oven at 353 K. Finally, the target product was obtained by calcination at 1073 K for 4 hours.[15]

C_3N_4 was prepared using SiO_2 sphere as hard template. For the synthesis of SiO_2 sphere, L-lysine (0.292 g), n-octane (14.600 g) and 280 mL of deionized water were mixed in a 500 mL of flask under vigorously stirring at 333 K for 5 hours. Tetraethyl orthosilicate (20.820 g) was added to the solution, and then the mixture was kept stirring for 20 hours. Later, the mixed solution was transferred into Teflon lined stainless steel autoclaves and crystallized at 373 K for 20 hours. Finally, the mixture was directly evaporated in an oil bath at 373 K. The silica sphere was obtained by calcination at 873 K for 8 hours.[16] For the synthesis of C_3N_4, cyanamide (3.000 g) and SiO_2 sphere (4.500 g) were mixed together and then the resulting white powder was calcined at 550 °C for 4 hours under nitrogen flow. C_3N_4 was obtained after the calcined yellow product was etched by 200 mL of NH_4HF_2 solution (4 M) for 2 days.[17]

The first type of supported AuM NPs, which were labelled as AuM/NXC-1, AuM/C_3N_4-1 and AuM/XC-1, were prepared via in situ process using $NaBH_4$ and NH_3BH_3 as reductants. In a typical experiment, the process of preparing Au_1Co_7/NXC-1, Au_1Co_7/C_3N_4-1 and Au_1Co_7/XC-1 and their catalytic study was as follows: 4.7 mL of aqueous solution containing $HAuCl_4{\cdot}4H_2O$ (0.0043 mmol) and $CoCl_2{\cdot}2H_2O$ (0.030 mmol) were kept in a two-necked round-bottom flask (25 mL). One neck was connected to a gas burette for monitoring the evolution of gas, and the other was sealed with a rubber plug. Then, dehydrated NXC, C_3N_4 or XC (10 mg) was introduced to the solution and kept vigorously shaking for 4 hours. After that, 1.5 mL of aqueous solution with NH_3BH_3 (1.71 mmol) and $NaBH_4$ (0.068 mmol) was syringed into the flask through the rubber plug, and the H_2-generated reaction started immediately. The reaction was not completed until there was no more gas generated.

The second type of supported AuM NPs, which were labelled as AuM/NXC-2, AuM/C_3N_4-2 and AuM/XC-2 were prepared via an ex situ process using $NaBH_4$ as reductant. For Au_1Co_7/NXC-2, Au_1Co_7/C_3N_4-2 and Au_1Co_7/XC-2, the preparation procedure was the same as the in situ synthesized Au_1Co_7/NXC-1, Au_1Co_7/C_3N_4-1 and Au_1Co_7/XC-1 except the absence of NH_3BH_3 as reductant. Once the metal alloy NPs generated, the aqueous solution of NH_3BH_3 was then introduced into the above solution containing metal alloy NPs to study its catalytic hydrolysis reaction.

The third type of supported AuM NPs, which were labelled as AuM/NXC-3, AuM/C_3N_4-3 and AuM/XC-3 were prepared under the same conditions as in in situ synthesized AuM/NXC-1, AuM/C_3N_4-1 and AuM/XC-1 except that NH_3BH_3 was used as the reductant. Once NH_3BH_3 was added into the suspension containing metal precursors and support, the catalytic reaction immediately began.

The molar ratio for metal:NH_3BH_3 was kept a constant of 0.02:1 in all the catalytic processes. The reactions were performed at different temperatures (298, 308, 313 and 323 K) with different catalysts under ambient atmosphere. The atmospheric pressure in Hohhot, Inner Mongolia was 88.8 kPa.

2.3 Recycle stability

Journal of Materials Chemistry A Accepted Manuscript

 This journal is © The Royal Society of Chemistry 20xx

Please do not adjust margins

After the first hydrogen generation reaction completed, the aqueous solution containing equivalent NH_3BH_3 (1.14 M, 1.5 mL) was added into the reaction flask. The evolution of gas was monitored using the gas burette. Such cycle experiments were repeated for 5 times under ambient atmosphere at room temperature.

2.4 Characterization

Powder X-ray diffraction (XRD) measurements were performed on a Panalytical X-Pert X-ray diffractmeter with a Cu-Kα source (40 kV, 20 mA). The X-ray photoelectron spectra (XPS) analyses were carried out on an ESCALAB250 (Thermo VG Corp.) equipped with an Al-Kα X-ray excitation source (1486.6 eV) that operated at 15 kV and 20 mA. The surface area measurements were performed with N_2 adsorption/desorption isotherms at 77 K after dehydration under vacuum at 150 °C for 12 h using automatic volumetric adsorption equipment (Autosorb-iQ2-MP). The transmission electron microscope (TEM, JEM-2010) equipped with an energy dispersive X-ray spectrometer (EDS) for elemental analysis was applied for the morphologies and composition of the as-synthesized samples. TEM samples were prepared by depositing two droplets of the catalyst suspensions onto amorphous carbon-coated copper grids. The IR spectra were recorded on an infrared spectrometer (Thermo Fisher Scientific, NEXUS-670) in the wavenumber range from 400-4000 cm^{-1}. The C, H and N contents in the samples were measured by an elemental analyser (Vario EL CHNOS).

2.5 Calculation method

The turnover frequency (TOF) reported here was a total TOF value based on the number of metal atoms in the surface of catalyst, which was calculated from the equation as follow:

$$TOF = \frac{3C_{AB}}{C_{surf}t}$$

(with units of mol-H_2 per mol-surface-atom per min), where C_{AB} was the total concentration of AB in the reactor, C_{surf} is the total surface metals content in the reactor, and t is the reaction time.[18] If the average size of well-dispersed AuCo nanoparticles is less than 5.0 nm, all the Au and Co species in the AuCo nanoparticles can be assumed as the total surface metal atoms participating the catalytic reaction.

3. Results and discussion

3.1 Catalyst characterization

In order to explore the effect of different supports on the catalytic activity of hydrolytic dehydrogenation of NH_3BH_3, two N-doped carbon materials, NXC and C_3N_4, were selected to immobilize bimetallic NPs (Fig. 1). In addition, three reduction ways towards mixed metal ions $AuCl_4^-$ and M^{2+}, namely in situ reduction by $NaBH_4$ and NH_3BH_3, ex situ reduction by $NaBH_4$ and in situ reduction by NH_3BH_3, were selected to construct and tune bimetallic NPs with different morphologies.

TEM and EDS were employed to characterize the microstructures and compositions of AuCo NPs immobilized by NXC and C_3N_4. As shown in Fig. 2, the AuCo NPs were well dispersed on NXC and C_3N_4, and the average sizes of AuCo NPs in AuCo/NXC-1, AuCo/NXC-2, AuCo/NXC-3, AuCo/C_3N_4-1, AuCo/C_3N_4-2 and AuCo/C_3N_4-3 were 3.3 ± 0.5, 3.5 ± 0.7, 3.5 ± 0.5, 2.6 ± 0.3, 2.8 ± 0.4 and 2.1 ± 0.2 nm, respectively. From these results, it can be clearly observed that the AuCo NPs had high dispersion and there were different sizes of AuCo NPs in different supported catalysts. In comparison with AuCo NPs immobilized by NXC, AuCo NPs immobilized by C_3N_4 had smaller sizes, which was in accordance with the results observed from XRD patterns as bellow. These differences in the morphologies of bimetallic NPs may lead to different catalytic performance on hydrolysis of NH_3BH_3. The EDS spectra showed the presence of Au and Co in the six AuCo catalysts (Figs. S1 and S2). In order to compare the immobilization ability of different supports (N-doped carbon and N-free carbon) for metal NPs, the TEM measurements of AuCo/XC-1, AuCo/XC-2 and AuCo/XC-3 were performed. The results showed that most of the AuCo NPs leached from the surface of XC (Figs. S3), indicating the weak interaction between the bimetallic NPs and the carbon surface, which leaded to the poor catalytic activities as bellow.

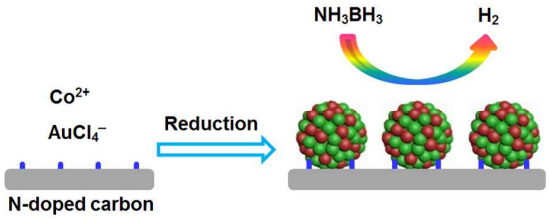

Fig. 1 Schematic illustration for preparation of bimetallic NPs immobilized by nitrogen-doped carbon support for catalytic H_2 generation from NH_3BH_3.

The XRD patterns of AuCo NPs immobilized by NXC and C_3N_4 showed that a peak around 38.2° corresponding to the d (111) of the cubic metallic Au was observed and no diffractions of Co species were found (Figs. S5 and S6), implying that Co species existed in an amorphous state in all the bimetallic catalysts, which was similar to the previous reports.[19] It should be noted that in comparison with AuCo NPs immobilized by NXC, the peaks corresponding to metallic Au in AuCo NPs immobilized by C_3N_4 were broader, demonstrating that AuCo NPs immobilized by C_3N_4 had smaller sizes and dispersed more uniformly on the supports, as also indicated by the TEM results. In addition, compared to bimetallic AuCo catalysts, the corresponding monometallic Au catalysts showed stronger characteristic peaks of Au, possible due to the larger size or the good crystallization of Au nanoparticles (Figs. S7 and S8). In order to determine the difference in the amorphous state of Co species in the catalysts, we analyzed the XRD patterns of AuCo/NXC-1, AuCo/NXC-2, AuCo/NXC-3, AuCo/C_3N_4-1, AuCo/C_3N_4-2 and AuCo/C_3N_4-3 samples after heating at 873 and 1173 K in Ar atmosphere (Figs. S5 and S6). The results showed that after heat treatment of the six catalysts at 873 K for 4 h, the Co species in AuCo/NXC-1 and AuCo/NXC-2 was

Journal of Materials Chemistry A Accepted Manuscript

crystallized into metallic Co and the Co species in AuCo/C_3N_4-1 was crystallized into CoO, while the Co species in AuCo/NXC-3, AuCo/C_3N_4-2 and AuCo/C_3N_4-3 still kept the amorphous state. When the temperature was raised to 1173 K, the Co species in AuCo/NXC-3, AuCo/C_3N_4-1 and AuCo/C_3N_4-2 was also crystallized into metallic Co. These phenomena suggested that existence states of Co species in these catalysts were different.

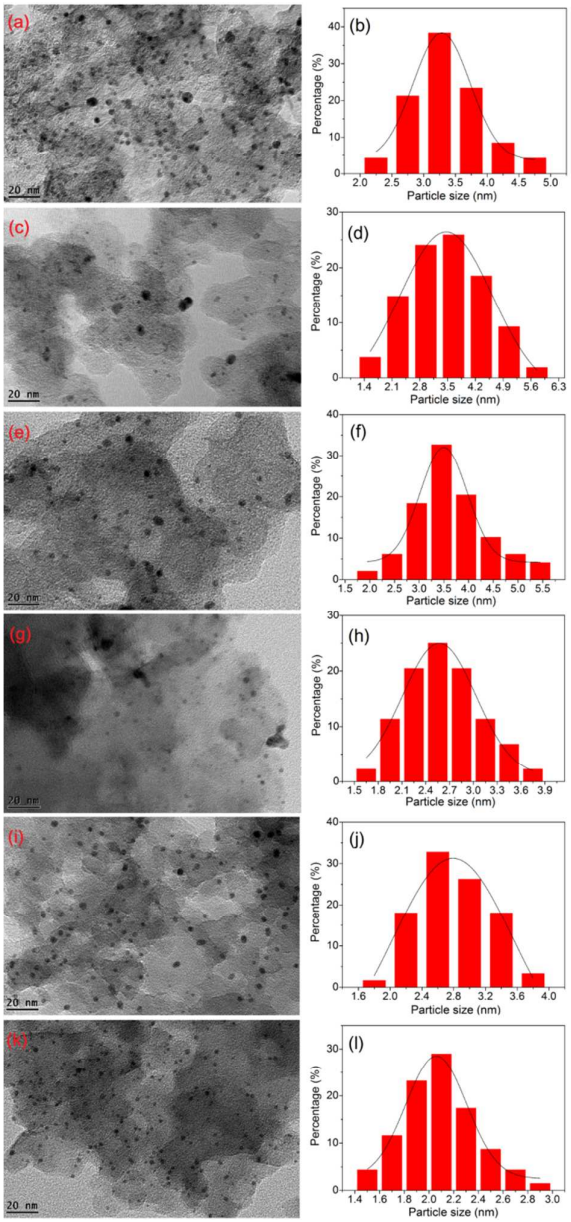

Fig. 2 Representative TEM images and corresponding distribution size histograms of (a, b) AuCo/NXC-1, (c, d) AuCo/NXC-2, (e, f) AuCo/NXC-3, (g, h) AuCo/C_3N_4-1, (i, j) AuCo/C_3N_4-2 and (k, l) AuCo/C_3N_4-3 (Au/Co = 1/7).

The element analysis showed that the content of N in NXC is 1.26 wt%. From the IR spectra (Figs. S10 and S11), it could be concluded that that nitrogen atoms were doped in the as-synthesized supports NXC and C_3N_4 and the frameworks of supports maintained the integrity in the resulting catalysts.[10] The N_2 absorption/desorption measurements showed that the Brunauer-Emmertt-Teller (BET) surface areas of NXC, AuCo/NXC -1, AuCo/NXC-2, AuCo/NXC-3, C_3N_4, AuCo/C_3N_4-1, AuCo/C_3N_4-2 and AuCo/C_3N_4-3 were 111.790, 86.575, 84.286, 92.314, 190.155, 166.942, 169.319 and 185.669 $cm^3 \cdot g^{-1}$, respectively. The appreciable decrease in the amount of N_2 adsorption of bimetallic catalysts indicated that the channels of NXC and C_3N_4 were occupied by AuCo NPs and/or blocked by the AuCo NPs located at their surface (Figs. S12 and S13). The X-ray photoelectron spectrometry (XPS) investigation before and after Ar etching was conducted for AuCo catalysts (Figs. 3 and S15). The results showed that the peaks of metallic Au species were found both before and after Ar etching, while the peaks of metallic Co species were detected after Ar etching. Moreover, the peaks of only oxidized Co species were found before Ar etching, which could be ascribed to the oxidation of metallic Co in the surface of AuCo NPs in the catalysts separated from the aqueous suspension. The observed peaks of Au and Co species in the XPS patterns of the catalysts indicated the existence of bimetallic alloy structures in the catalysts.[20]

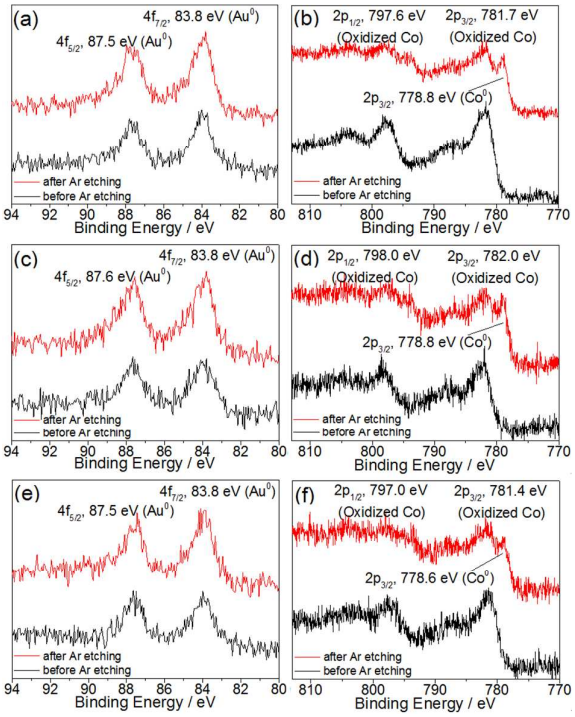

Fig. 3 XPS spectra for (a, b) AuCo/NXC-1, (c, d) AuCo/NXC-2 and (e, f) AuCo/NXC-3 (Au/Co = 1/7) before and after Ar etching.

3.2 Catalytic activity

3.2.1 Effect of support types

In order to explore the catalytic behaviors of bimetallic NPs immobilized by the two types of porous N-doped carbon supports, catalytic H_2 generation from hydrolysis of NH_3BH_3 were tested. As shown in Fig. 4, AuCo/C_3N_4-1 had a high capability for dehydrogenation of NH_3BH_3. Surprisingly,

This journal is © The Royal Society of Chemistry 20xx

Please do not adjust margins

Journal of Materials Chemistry A Accepted Manuscript

compared to AuCo/C_3N_4-1, AuCo/NXC-1 exhibited the remarkably enhanced activity with a total turnover frequency (TOF) value of 42.1 $mol_{H2}{\cdot}mol_{cat}^{-1}{\cdot}min^{-1}$, among the highest values ever reported under the similar conditions (Table S1). In general, the small size of metal NPs is beneficial for the catalytic performance, especially activity.[21] Nevertheless, AuCo/NXC-1 featuring small size (3.3 ± 0.5 nm) of AuCo NPs had much higher activity than AuCo/C_3N_4-1 featuring small size (2.6 ± 0.3 nm) of AuCo NPs, which indicated that the different N-doped carbon materials as supports for immobilizing bimetallic catalysts had a significant effect on the catalytic activities. This may also be explained that compared with the delocalized electron in nitrogen in C_3N_4 with graphite layered structure, the electron in nitrogen in NXC was more easily transferred to AuCo NPs, and then the electron density of AuCo NPs immobilized by NXC was enhanced, leading to the high activity of AuCo/NXC-1 for hydrolysis of NH_3BH_3.

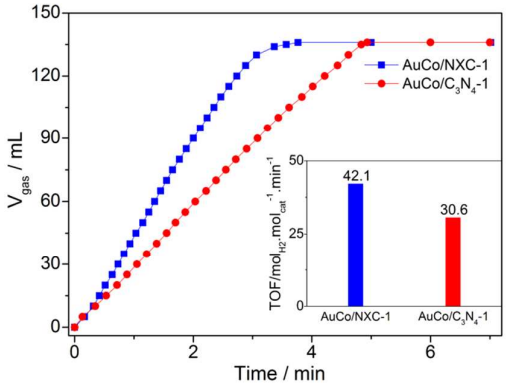

Fig. 4 Plots of time versus volume of H_2 generated from aqueous NH_3BH_3 (0.276 M, 6.2 mL) over AuCo/NXC-1 and AuCo/C_3N_4-1 at room temperature.

3.2.2 Effect of reduction methods

Different bimetallic NPs with different microstructures played an important role in the catalysis.[7e] So the activities of AuCo/NXC-1, AuCo/NXC-2 and AuCo/NXC-3 synthesized using different reductants were investigated. The results showed that AuCo/NXC-1 prepared via in situ reduction by $NaBH_4$ and NH_3BH_3 displayed the highest activity among the three catalysts, and AuCo/NXC-2 prepared via ex situ reduction by $NaBH_4$ displayed the lowest activity (Fig. 5a). In the C_3N_4-immobilized bimetallic catalysts, the activities were in the order of AuCo/C_3N_4-1 > AuCo/C_3N_4-3 > AuCo/C_3N_4-2 (Fig. 5b). From the above catalytic results of the six AuCo catalysts, it could be concluded that the synergistic effect of supports and AuCo NPs with different microstructures played an import role in catalytic activity in the hydrolysis of NH_3BH_3, resulting in the highest activity of NXC-immobilized AuCo catalyst AuCo/NXC-1. In order to confirm the contribution of N-doping in supports to the catalytic dehydrogenation of aqueous NH_3BH_3, the activities of bare XC and N-doped XC (NXC)-immobilized AuCo NPs were compared. The results showed that the bare XC-based catalysts featured lower activities than N-doped XC-based catalysts prepared using the same synthesis method (Fig. 6), indicating that the N-doped carbon supports played an important role in the enhanced activity in hydrolysis of NH_3BH_3. In addition, the large sizes of AuCo nanoparticles in XC-based AuCo catalysts might lead to their low activities (Fig. S3).

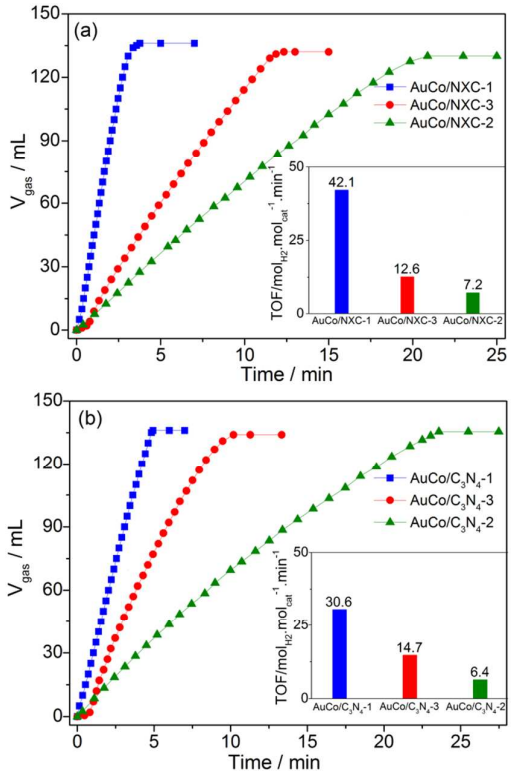

Fig. 5 Plots of time versus volume of H_2 generated from aqueous NH_3BH_3 (0.276 M, 6.2 mL) over (a) NXC-immobilized AuCo catalysts and (b) C_3N_4-immobilized AuCo catalysts at room temperature.

3.2.3 Effect of metal components

Besides the microstructures, the components of active metal NPs remarkably influenced their activities.[7j,7k] In view of this, the activities of NXC and C_3N_4-immobilized AuNi nanocatalysts were tested. The results showed that they displayed remarkably different activities, and their orderliness of activities was different from that of the corresponding AuCo catalysts. The AuNi catalysts were ordered in terms of catalytic activity: AuNi/NXC-3 > AuNi/NXC-1 > AuNi/NXC-2 (Fig. S16) and AuNi/C_3N_4-1 > AuNi/C_3N_4-3 > AuNi/C_3N_4-2 (Fig. S17). From this phenomenon, it can be seen that as a whole, the activities of AuCo catalysts were superior to AuNi catalysts, which could be attributed to the more excellent activity of Co NPs than that of Ni NPs toward hydrogen generation from NH_3BH_3. In addition, the activities of AuCo/NXC-1 and AuCo/C_3N_4-1 had remarkable change when the ratio of Au/Co was greatly tuned (Figs. S18 and S19), which was similar to the reported bimetallic catalysts for hydrolysis of NH_3BH_3.[7h,7n,20] More importantly, this tendency is beneficial for the remarkable

Journal of Materials Chemistry A Accepted Manuscript

decrease in the amount of noble metals in the catalysts. Compare to the remarkable change with tuning the ratio of Au/Co in the activities of AuCo/NXC-1 and AuCo/C_3N_4-1 prepared via in situ reduction by $NaBH_4$ and NH_3BH_3, AuCo/NXC-3 and AuCo/C_3N_4-3 prepared via in situ reduction by NH_3BH_3 exhibited no significantly change in the activities with the change of Au/Co (Figs. S20 and S21), which indicated that the different reductants towards $AuCl_4^-$ and Co^{2+} may play an different role in constructing AuCo NPs with different microstructures, resulting in different catalytic activities.

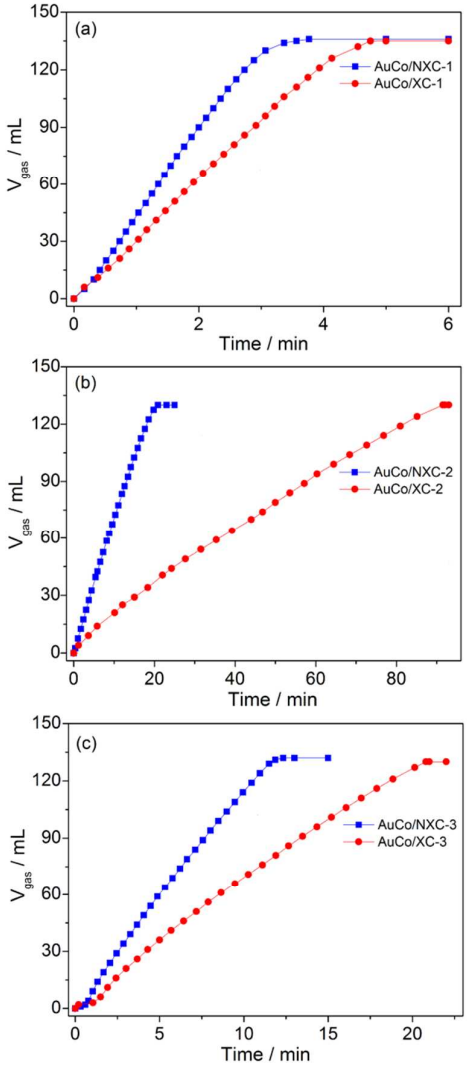

Fig. 6 Plots of time versus volume of H_2 generated from aqueous NH_3BH_3 (0.276 M, 6.2 mL) over (a) AuCo/NXC-1 and AuCo/XC-1, (b) AuCo/NXC-2 and AuCo/XC-2 and (c) AuCo/NXC-3 and AuCo/XC-3 at room temperature.

3.3 Activation energy

Temperature plays an important role in the process of NH_3BH_3 hydrolysis.[22] The catalytic dehydrogenation rates of NXC and C_3N_4-immobilized AuCo catalysts towards the aqueous NH_3BH_3 at different temperatures were investigated (Figs. 7 and S22). The results showed that the H_2 generation rate rose sharply when the temperature increased from 298 to 323 K, indicating that a high reaction temperature was beneficial for enhancing the dehydrogenation rate of NH_3BH_3. According to the Arrhenius plot, the obtained apparent activation energy (E_a) of the dehydrogenation of NH_3BH_3 involving AuCo/NXC-1, AuCo/NXC-2 and AuCo/NXC-3 were calculated to be 31.92, 46.22 and 50.15 kJ/mol, respectively. Among these values, the E_a value of AuCo/NC-1 was the lowest and was lower than most of the reported values even with noble-metal catalysts.[23] In addition, the E_a value of AuCo/C_3N_4-1 was 40.91 kJ/mol, which was higher than AuCo/NXC-1, but was still lower than the reported values for the same reaction using various catalysts.[24]

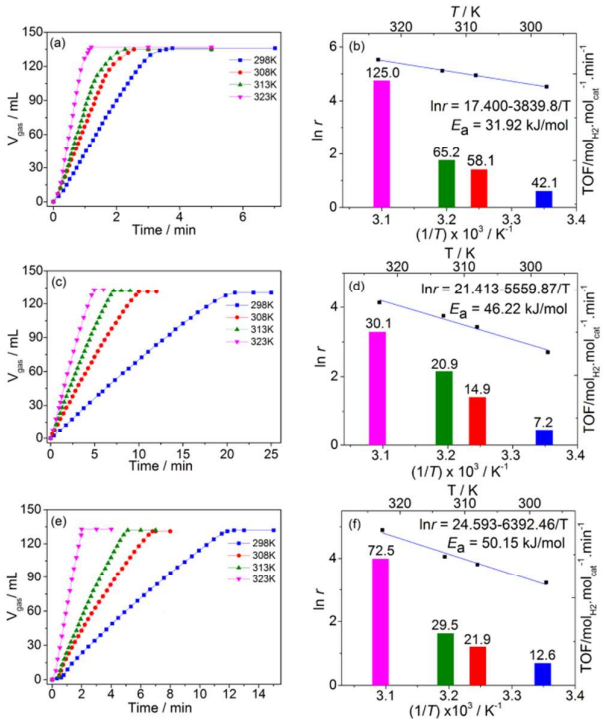

Fig. 7 Plots of time versus volume of H_2 generated from aqueous NH_3BH_3 (0.276 M, 6.2 mL) and Arrhenius plots and TOF values of NH_3BH_3 dehydrogenation over (a, b) AuCo/NXC-1, (c, d) AuCo/NXC-2 and (e, f) AuCo/NXC-3 (Au/Co = 1/7) at different temperatures.

3.4 Recycle stability

The recycle stability is of crucial importance on the practical application of catalysts, so the durability tests of AuCo/NXC-1, AuCo/NXC-2 and AuCo/NXC-3 were carried out at room temperature. As shown in Fig. 8, even after 5 runs, the productivity of H_2 remained almost unchanged, indicating that the three supported bimetallic catalysts had long durability, which can be attributed to the formation of bimetallic NPs immobilized by N-doped carbon supports. Compared to the stable activities of AuCo/NXC-2 and AuCo/NXC-3, the activity of AuCo/NXC-1 after the first run was lowered; however, its activity kept constantly in the rest runs. This phenomenon was

Journal of Materials Chemistry A Accepted Manuscript

This journal is © The Royal Society of Chemistry 20xx

Please do not adjust margins

likely to result from the metastable state of AuCo alloy NPs prepared via in situ reduction way.

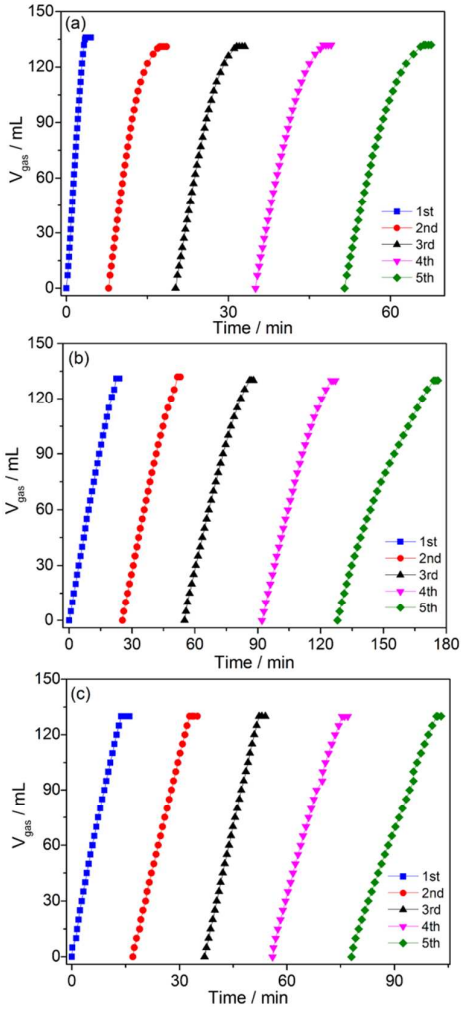

Fig. 8 Durability test for H_2 generated from aqueous NH_3BH_3 over as-synthesized catalysts after addition of the same amount of NH_3BH_3 (1.71 mmol) at room temperature: (a) AuCo/NXC-1, (b) AuCo/NXC-2 and (c) AuCo/NXC-3 (Au/Co = 1/7).

Conclusions

In summary, two N-doped carbon materials with different structures were used as supports to prepare a series of surfactant-free AuM (M = Co, Ni) NPs through three different reduction ways towards mixed metal ions, which exhibited remarkably different catalytic activities for hydrolysis of NH_3BH_3. Among all the bimetallic NPs, the NXC-immobilized AuCo alloy NPs in situ synthesized using $NaBH_4$ and NH_3BH_3 as reductant exhibited superior catalytic activity featuring a TOF value of 42.1 $mol_{H2}{\cdot}mol_{cat}^{-1}{\cdot}min^{-1}$. The interaction between the N-doped NXC and in situ synthesized AuCo NPs played an important role for the highly efficient activation of N-B bond in NH_3BH_3. In addition, the as-synthesized catalysts exhibited high recycle stability. Through designing and selecting porous functionalized materials as supports to tune the interactions between supports and active metal NPs with different structures, it is possible to design high-performance nanocatalysts that are important for sustainable energy production and chemical synthesis applications.

Acknowledgements

The authors gratefully acknowledge financial support from the Program for New Century Excellent Talents in University of the Ministry of Education of China (grant no. NCET-13-0846), the National Natural Science Foundation of China (grant no. 21101089), the Inner Mongolia Natural Science Foundation (grant no. 2011JQ01), the Program for Young Talents of Science and Technology in Universities of Inner Mongolia Autonomous Region (grant no. NJYT-13-A01), the Program for the Development of Innovative Teams in Universities of Inner Mongolia (grant no. NMGIRT1105), and the Program for Science and technology leading talent and innovation team of Inner Mongolia (grant no. 209182).

References

1 (*a*) M. S. Dresselhaus and I. L. Thomas, *Nature*, 2001, **414**, 332–337; (*b*) P. Chen, Z. Xiong, J. Luo, J. Lin and K. L. Tan, *Nature*, 2002, **420**, 302–304; (*c*) P. P. Edwards, V. L. Kuznetsov, W. I. David and N. P. Brandon, *Energy Policy*, 2008, **36**, 4356–4362.

2 (*a*) L. Schlapbach and A. Züttel, *Nature*, 2001, **414**, 353–358; (*b*) J. A. Turner, *Science*, 2004, **305**, 972–974; (*c*) W. Grochala and P. P. Edwards, *Chem. Rev.*, 2004, **104**, 1283–1315; (*d*) G. W. Huber, S. Iborra and A. Corma, *Chem. Rev.*, 2006, **106**, 4044–4098; (*e*) A. Staubitz, A. P. M. Robertson and I. Manners, *Chem. Rev.*, 2010, **110**, 4079–4124; (*f*) Y. H. Hu and L. Zhang, *Adv. Mater.*, 2010, **22**, E117–E130; (*g*) X. Gu, Z.-H. Lu, H.-L. Jiang, T. Akita and Q. Xu, *J. Am. Chem. Soc.*, 2011, **133**, 11822–11825; (*h*) Y.-Y. Cai, X.-H. Li, Y.-N. Zhang, X. Wei, K.-X. Wang and J.-S. Chen, *Angew. Chem., Int. Ed.*, 2013, **52**, 11822 –11825.

3 (*a*) W. Lubitz and W. Tumas, *Chem. Rev.*, 2007, **107**, 3900–3903; (*b*) R. M. Navarro, M. A. Pena and J. L. G. Fierro, *Chem. Rev.*, 2007, **107**, 3952–3991; (*c*) V. V. Struzhkin, B. Militzer, W. L. Mao, H. Mao and R. J. Hemley, *Chem. Rev.*, 2007, **107**, 4133–4151; (d) Q.-L. Zhu and Q. Xu, *Energy Environ. Sci.*, 2015, **8**, 478–512.

4 (*a*) A. Gutowska, L. Li, Y. Shin, C. M. Wang, X. S. Li, J. C. Linehan, R. S. Smith, B. D. Kay, B. Schmid, W. Shaw, M. Gutowski and T. Autrey, *Angew. Chem., Int. Ed.*, 2005, **44**, 3578–3582; (*b*) Y. Chen, J. L. Fulton, J. C. Linehan and T. Autrey, *J. Am. Chem. Soc.*, 2005, **127**, 3254–3255; (*c*) B. Peng and J. Chen, *Energy Environ. Sci.*, 2008, **1**, 479–483; (*d*) Z. Xiong, C. K. Yong, G. T. Wu, P. Chen, W. Shaw, A. Karkamkar, T. Autrey, M. O. Jones, S. R. Johnson, P. P. Edwards and W. I. F. David, *Nat. Mater.*, 2008, **7**, 138–141; (*e*) C. W. Hamilton, R. T. Baker, A. Staubitz and I. Manners, *Chem. Soc. Rev.*, 2009, **38**, 279–293; (*f*) B. L. Davis, D. A. Dixon, E. B. Garner, J. C. Gordon, M. H. Matus, B. Scott and F. H. Stephens. *Angew. Chem., Int. Ed.*, 2009, **48**, 6812–6816.

5 (*a*) M. Chandra and Q. Xu, *J. Power Sources*, 2006, **156**, 190–194; (*b*) D. J. Heldebrant, A. Karkamkar, N. J. Hess, M. Bowden, S. Rassat, F. Zheng, K. Rappe and T. Autrey, *Chem. Mater.*, 2008, **20**, 5332–5336; (*c*) M. Diwan, V. Diakov, E.

Journal of Materials Chemistry A Accepted Manuscript

Shafirovich and A. Varma, *Int. J. Hydrogen Energy*, 2008, **33**, 1135–1141; (*d*) U. B. Demirci and P. Miele, *Energy Environ. Sci.*, 2009, **2**, 627–637; (*e*) Ö. Metin, V. Mazumder, S. Özkar and S. Sun, *J. Am. Chem. Soc*., 2010, **132**, 1468–1469; (*f*) H.-L. Jiang and Q. Xu, *Catal. Today*, 2011, **170**, 56–63; (*g*) Z. Tang, X. Chen, H. Chen, L. Wu and X. Yu, *Angew. Chem., Int. Ed.*, 2013, **52**, 5832–5835.

6 (*a*) M. Chandra and Q. Xu, *J Power Sources*, 2007, **168**, 135–142; (*b*) N. Blaquiere, S. Diallo-Garcia, S. I. Gorelsky, D. A. Black and K. Fagnou, *J. Am. Chem. Soc.*, 2008, **130**, 14034–14035; (*c*) T. He, Z. Xiong, G. Wu, H. Chu, C. Wu, T. Zhang and P. Chen, *Chem. Mater*., 2009, **21**, 2315–2318; (*d*) S.-K. Kim, W.-S. Han, T.-J. Kim, T.-Y. Kim, S. W. Nam, M. Mitoraj, L. Piekos, A. Michalak, S.-J. Hwang and S. O. Kang, *J. Am. Chem. Soc.*, 2010, **132**, 9954–9955; (*e*) D.-H. Sun, V. Mazumder, Ö. Metin and S. Sun, *ACS Nano*, 2011, **5**, 6458–6464; (*f*) G. Chen, S. Desinan, R. Rosei, F. Rosei and D. Ma, *Chem. Commun.*, 2012, **48**, 8009–8011; (*g*) F. Qiu, L. Li, G. Liu, Y. Wang, C. An, C. Xu, Y. Xu, Y. Wang, L. Jiao and H. Yuan, *Int. J. Hydrogen Energy*, 2013, **38**, 7291–7297.

7 (*a*) F. Tao, M. E. Grass, Y. Zhang, D. R. Butcher, J. R. Renzas, Z. Liu, J. Y. Chung, B. S. Mun, M. Salmeron and G. A. Somorjai, *Science*, 2008, **322**, 932–934; (*b*) X. Yang, F. Cheng, J. Liang, Z. Tao and J. Chen, *Int. J. Hydrogen Energy*, 2009, **34**, 8785–8791; (*c*) H.-L. Jiang, T. Umegaki, T. Akita, X.-B. Zhang, M. Haruta and Q. Xu, *Chem. Eur. J.*, 2010, **16**, 3132–3137; (*d*) J.-M. Yan, X.-B. Zhang, T. Akita, M. Haruta, and Q. Xu, *J. Am. Chem. Soc.*, 2010, **132**, 5326–5327; (*e*) H.-L. Jiang and Q. Xu, *J. Mater. Chem*., 2011, **21**, 13705–13725; (*f*) X. Yang, F. Cheng, J. Liang, Z. Tao and J. Chen, *Int. J. Hydrogen Energy*, 2011, **36**, 1984–1990; (*g*) G. Chen, S. Desinan, R. Nechache, R. Rosei, F. Rosei and D. Ma, *Chem. Commun.*, 2011, **47**, 6308–6310; (*h*) H.-L. Jiang, T. Akita and Q. Xu, *Chem. Commun.*, 2011, **47**, 10999–11001; (*i*) G. Chen, S. Desinan, R. Rosei, F. Rosei and D. Ma, *Chem. Eur. J.*, 2012, **18**, 7925–7930; (*j*) F. Tao, *Chem. Soc. Rev.*, 2012, **41**, 7977–7979; (*k*) Z. Wei, J. Sun, Y. Li, A. K. Datye and Y. Wang, *Chem. Soc. Rev*., 2012, **41**, 7994–8008; (*l*) F. Gao and D. W. Goodman, *Chem. Soc. Rev.*, 2012, **41**, 8009–8020; (*m*) M. Sankar, N. Dimitratos, P. J. Miedziak, P. P. Wells, C. J. Kiely and G. J. Hutchings, *Chem. Soc. Rev.*, 2012, **41**, 8099–8139; (*n*) Z.-H. Lu, J. Li, A. Zhu, Q. Yao, W. Huang, R. Zhou, R. Zhou and X. Chen, *Int. J. Hydrogen Energy*, 2013, **38**, 5330–5337; (*o*) N. Cao, J. Su, W. Luo and G. Z. Cheng, *Catal. Commun.*, 2014, **43**, 47–51; (*p*) Q. Zhang, I. Lee, J. B. Joo, F. Zaera and Y. Yin, *Acc. Chem. Res.*, 2013, **46**, 1816–1824; (*q*) N. Cao, K. Hu, W. Luo and G. Cheng, *J. Alloys Comp.*, 2014, **590**, 241–246; (*r*) X. Li, C. Zeng and G. Fan, *Int. J. Hydrogen Energy*, 2015, **40**, 9217–9224; (*s*) X. Li, C. Zeng and G. Fan, *Int. J. Hydrogen Energy*, 2015, **40**, 3883–3891; (*t*) Q. Yao, Z.-H. Lu, Y. Wang, X. Chen and G. Feng, *J. Phys. Chem. C*, 2015, **119**, 14167–14174; (*u*) A. Bulut, M. Yurderi, İ. E. Ertas, M. Celebi, M. Kaya and M. Zahmakiran, *Appl. Catal. B: Environ.*, 2016, **180**, 121–129.

8 (*a*) P. Z. Li, A. Aijaz and Q. Xu, *Angew. Chem., Int. Ed.*, 2012, **51**, 6753–6756; (*b*) Q.-L. Zhu, J. Li and Q. Xu, *J. Am. Chem. Soc.*, 2013, **135**, 10210–10213.

9 (*a*) M. Chandra and Q. Xu, *J. Power Sources*, 2007, **168**, 135–142; (*b*) H. L. Jiang, T. Akita, T. Ishida, M. Haruta and Q. Xu, *J. Am. Chem. Soc.*, 2011, **133**, 1304–1306; (*c*) J.-M. Yan, Z.-L. Wang, H.-L. Wang and Q. Jiang, *J. Mater. Chem.*, 2012, **22**, 10990–10993; (*d*) J. Wang, Y.-L. Qin, X. Liu and X.-B. Zhang, *J. Mater. Chem.*, 2012, **22**, 12468–12470; (*e*) J. Li, Q.-L. Zhu and Q. Xu, *Catal. Sci. Technol.*, 2015, **5**, 525–530.

10 L.-T. Guo, Y.-Y. Cai, J.-M. Ge, Y.-N. Zhang, L.-H. Gong, X.-H. Li, K.-X. Wang, Q.-Z. Ren, J. Su and J.-S. Chen, *ACS Catal.*, 2015, **5**, 388–392.

11 (*a*) J.-M. Yan, X.-B. Zhang, S. Han, H. Shioyama and Q. Xu, *Inorg. Chem.*, 2009, **48**, 7389–7393; (*b*) P.-Z. Li, K. Aranishi and Q. Xu, *Chem. Commun.*, 2012, **48**, 3173–3175; (*c*) H. R. Moon, D.-W. Lim and M. P. Suh, *Chem. Soc. Rev.*, 2013, **42**, 1807–1824.

12 (*a*) C. Liang, Z. Li and S. Dai, *Angew. Chem., Int. Ed.*, 2008, **47**, 3696–3717; (*b*) Y. Zhai, Y. Dou, D. Zhao, P. F. Fulvio, R. T. Mayes and S. Dai, *Adv. Mater.*, 2011, **23**, 4828–4850; (*c*) X. Xu, Y. Li, Y. Gong, P. Zhang, H. Li and Y. Wang, *J. Am. Chem. Soc.*, 2012, **134**, 16987–16990; (*d*) Y. Xia, Z. Yang and Y. Zhu, *J. Mater. Chem. A*, 2013, **1**, 9365–9381; (*e*) L. Wang, Z. Schnepp and M. M. Titirici, *J. Mater. Chem. A*, 2013, **1**, 5269–5273; (*f*) D. S. Su, S. Perathoner and G. Centi, *Chem. Rev.*, 2013, **113**, 5782–5816; (*g*) K. Chen, S. Song and D. Xue, *J. Mater. Chem. A*, 2015, **3**, 2441–2453; (*h*) J. Tang, J. Liu, C. Li, Y. Li, M. O. Tade, S. Dai and Y. Yamauchi, *Angew. Chem., Int. Ed.*, 2015, **54**, 588–593; (*i*) M. M. Titirici, R. J. White, N. Brun, V. L. Budarin, D. S. Su, F. del Monte, J. C. Clark and M. J. MacLachlan, *Chem. Soc. Rev.*, 2015, **44**, 250–290.

13 (*a*) Z. Li, J. Liu, Z. Huang, Y. Yang, C. Xia, and F. Li, *ACS Catal.*, 2013, **3**, 839–845; (*b*) M. Tang, S. Mao, M. Li, Z. Wei, F. Xu, H. Li and Y. Wang, *ACS Catal*., 2015, **5**, 3100–3107.

14 (*a*) L. S. Ott and R. G. Finke, *Chem. Rev.*, 2007, **251**, 1075–1100; (*b*) K. K. R. Datta, B. V. Subba Reddy, K. Ariga and A. Vinu, *Angew. Chem., Int. Ed.*, 2010, **49**, 5961–5965; (*c*) Z. Li, J. Liu, C. Xia and F. Li, *ACS Catal.*, 2013, **3**, 2440–2448; (*d*) X.-H. Li and M. Antonietti, *Chem. Soc. Rev.*, 2013, **42**, 6593–6604.

15 K. Lee, L. Zhang, H. Lui, R. Hui, Z. Shi and J. Zhang, *Electrochim. Acta*., 2009, **54**, 4704–4711.

16 T. Yokoi, Y. Sakamoto, O. Terasaki, Y. Kubota, T. Okubo and T. Tatsumi, *J. Am. Chem. Soc.*, 2006, **128**, 13664–13665.

17 (*a*) Y. Wang, J. Yao, H. Li, D. Su and M. Antonietti, *J. Am. Chem. Soc.*, 2011, **133**, 2362–2365; (*b*) Y. Zheng, Y. Jiao, J. Chen, J. Liu, J. Liang, A. Du, W. Zhang, Z. Zhu, S. C. Smith, M. Jaroniec, G. Q. Lu and S. Z. Qiao, *J. Am. Chem. Soc.*, 2011, **133**, 20116–20119; (*c*) J. Zhang, M. Zhang, C. Yang and X. Wang, *Adv. Mater.*, 2014, **26**, 4121–4126.

18 (*a*) Z. Zhao, Y-L. Fang, P. J. J. Alvarez and M. S. Wong, *Appl. Catal. B: Environ.*, 2013, **140-141**, 468–477; (*b*) Z. Zhao, J. Arentz, L. A. Pretzer, P. Limpornpipat, J. M. Clomburg, R. Gonzalez, N. M. Schweitzer, T. Wu, J. T. Miller and M. S. Wong, *Chem. Sci.*, 2014, **5**, 3715–3728; (*c*) H. Qian, Z. Zhao, J. C. Velazquez, L. A. Pretzer, K. N. Heck and M. S. Wong, *Nanoscale*, 2014, **6**, 358–364; (*d*) Z. Zhao, J. T. Miller, T. Wu, N. M. Schweitzer and M. S. Wong, *Top. Catal*., 2015, **58**, 302–313.

19 (*a*) J.-M. Yan, X.-B. Zhang, H. Shioyama and Q. Xu, *J. Power Sources*, 2010, **195**, 1091–1094; (*b*) Z.-H. Lu, H.-L. Jiang, M. Yadav, K. Aranishi and Q. Xu, *J. Mater. Chem*., 2012, **22**, 5065–5071; (*c*) L. Yang, W. Luo and G. Cheng, *ACS Appl. Mater. Interfaces*, 2013, **5**, 8231–8240; (*d*) J. Hu, Z. Chen, M. Li, X. Zhou and H. Lu, *ACS Appl. Mater. Interfaces*, 2014, **6**, 13191–13200.

20 J. Li, Q.-L. Zhu and Q. Xu, *Chem. Commun.*, 2014, **50**, 5899–5901.

21 (*a*) W. Chen, J. Ji, X. Feng, X. Duan, G. Qian, P. Li, X. Zhou, D. Chen and W. Yuan, *J. Am. Chem. Soc*., 2014, **136**, 16736–16739; (*b*) D. Gao, H. Zhou, J. Wang, S. Miao, F. Yang, G. Wang, J. Wang and X. Bao, *J. Am. Chem. Soc*., 2015, **137**, 4288–4291.

22 (*a*) Ö. Metin and S. Özkar, *Int. J. Hydrogen Energy*, 2011, **36**, 1424–1432; (*b*) F. Qiu, Y. Dai, L. Li, C. Xu, Y. Huang, C. Chen, Y. Wang, L. Jiao and H. Yuan, *Int. J. Hydrogen Energy*, 2014, **39**, 436–441.

23 (*a*) M. Rakap and S. Özkar, *Int. J. Hydrogen Energy*, 2010, **35**, 1305–1312; (*b*) H. Can and Ö. Metin, *Appl. Catal. B: Environ.*, 2012, **125**, 304–310.

24 (*a*) Q. Xu and M. Chandra, *J. Power Sources*, 2006, **163**, 364–370; (*b*) M. Rakap and S. Özkar, *Catal. Today*, 2012, **183**, 17–25.

Journal of Materials Chemistry A Accepted Manuscript

This journal is © The Royal Society of Chemistry 20xx

Please do not adjust margins

High-performance hydrogen generation from hydrolysis of ammonia borane has been achieved over porous nitrogen-doped carbon-immobilized bimetallic nanoparticles.

Journal of Materials Chemistry A Accepted Manuscript

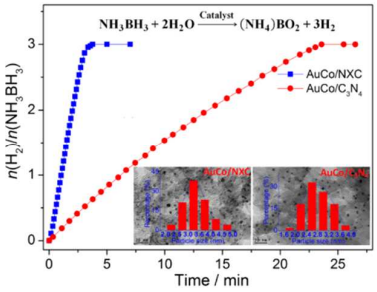

Journal of Materials Chemistry A Accepted Manuscript